ELKOMIKA: Jurnal Teknik Energi Elektrik, Teknik Telekomunikasi, & Teknik Elektronika

ISSN(p): 2338-8323 | ISSN(e): 2459-9638 | Vol. 14 | No. 3 | Halaman 347 – 357
DOI : http://dx.doi.org/10.26760/elkomika.v14i3.347 July 2026

Design of Microstrip-Embedded Building Structure Antenna for Smart City IoT Networks

Article History:
Received
5 May 2026
Revised
9 June 2026
Accepted
29 June 2026

LOMPO RAMOS EMAKARIM, NURMAYANTI ZAIN*, FARHAN REZKI ARIFIN, MUH. IRHAM M, UMMU KHALSUM, ABDUL HAKIM UDIN

Department of Electrical Engineering, University of Cokroaminoto Makassar, Tamalanrea-Makassar, Indonesia
*Email: nurmayanti.zain@ucm-si.ac.id

ABSTRAK

Teknologi antena terintegrasi bangunan merupakan pendekatan potensial untuk mendukung IoT di kota cerdas. Penelitian ini mengusulkan pemodelan konseptual antena mikrostrip tertanam dalam elemen struktur logam. Tujuannya adalah menganalisis perilaku elektromagnetik dan kinerja antena untuk aplikasi IoT. Metode penelitian menggabungkan pemodelan analitik dengan simulasi elektromagnetik HFSS untuk mengevaluasi parameter seperti return loss, VSWR, penguatan, dan pola radiasi pada pita frekuensi 700 MHz untuk jaringan IoT sub-GHz. Hasil simulasi menunjukkan struktur kolom beton dapat mendukung operasi antena dengan return loss -17,15 dB dan VSWR 1,32. Meskipun terdapat atenuasi, antena mempertahankan penguatan positif 1,44 dBi dengan radiasi broadside yang memadai. Simpulan studi mengonfirmasi antena tertanam ini layak untuk IoT infrastruktur kota cerdas.

***Kata kunci**: Antena Terintegrasi Bangunan, Antena Mikrostrip, IoT Sub-GHz, Infrastruktur Kota Cerdas, Pemodelan Konseptual*

ABSTRACT

Building-integrated antenna technology offers a promising approach for IoT deployment in smart city. This study proposes a conceptual framework for microstrip antenna embedded within metal structural elements. It aims to analyze the electromagnetic behavior and performance of these antennas for IoT applications. The methodology combines analytical modeling with HFSS simulations to evaluate key parameters including return loss, VSWR, gain, and radiation patterns within the 700 MHz sub-GHz IoT bands. Simulation results demonstrate that the concrete column structure supports effective antenna operation, achieving a return loss of -17.15 dB and a VSWR of 1.32. Despite the inherent attenuation, the antenna maintains a positive realized gain of 1.44 dBi and a sufficient broadside radiation pattern. The study concludes that such embedded antennas offer a viable solution for smart city IoT infrastructure.

***Keywords**: Building-Integrated Antenna, Microstrip Antenna, Sub-GHz IoT, Smart City Infrastructure, Conceptual Modeling*

1. INTRODUCTION

The accelerated expansion of smart city has created a pressing need for scalable and efficient Internet of Things (IoT) networks, which rely on pervasive sensing and communication infrastructures **(Mehboob, 2025) (Zanella et al., 2014)**. A critical component of these networks is the antenna system, which must ensure reliable data transmission while being seamlessly integrated into urban environments **(Vähä-Savo et al., 2025)**. Conventional antenna installations often face limitations related to space, aesthetics, and structural compatibility, particularly in dense urban areas **(Khan et al., 2024)**. Microstrip antennas, widely used for their compactness and low-profile design, offer promising solutions; however, they often suffer from limited bandwidth, gain, and integration challenges when deployed within building structures **(Jusoh et al., 2023) (Inclán-Sánchez, 2023) (Hussain et al., 2022)**.

This study addresses these challenges by proposing a conceptual modeling framework for microstrip-embedded building structure antenna. The main objective is to evaluate the feasibility and electromagnetic performance of antenna embedded into metal structural elements such as rebar within concrete columns, specifically targeting sub-GHz IoT networks **(Rita et al., 2025)**. The selection of the operational frequency range is crucial. In the context of LPWAN systems for smart city applications, the 700 MHz band becomes a specific focus of this research. Globally known as the Digital Dividend Band and reallocated from television broadcasting to mobile broadband services, this frequency in Indonesia is particularly important due to its superior propagation characteristics, enabling better penetration through structural obstacles (e.g., building walls) **(Pavlík et al., 2024) (Akyıldız & Durmaz, 2022)**, and achieving wider area coverage with lower energy compared to higher frequencies (e.g., 2.4 GHz or 5G bands) **(Curwen & Whalley, 2021)**. High signal range and penetration at 700 MHz are ideal for urban-scale IoT applications, where sensor devices are often located inside buildings, underground, or in remote locations. By testing building metallic structures at this frequency, this study directly assesses the feasibility of antenna integration to support non-standalone (NSA) 5G and IoT networks in dense Indonesian urban areas, making it highly relevant for national smart city implementations **(Andalisto et al., 2021)**.

By integrating communication functions directly into building infrastructure, the approach aims to provide scalable, low-visibility solutions. This study builds upon the conceptual analysis of transforming standard metal structural elements into functional communication systems **(Zain et al., 2025a) (Zain et al., 2025b)**. While previous work focused on the general performance of loop antenna systems within walls **(Arifin et al., 2025)**, this research specifically investigates the integration of microstrip patch within the carbon steel reinforcement. Previous research has explored various techniques to enhance microstrip antenna performance, including reconfigurable MIMO designs for IoT wireless applications **(Kumar et al., 2024)**, wideband bow-tie slot antennas embedded in dielectric materials for 5G communication **(Chen & Zheng, 2023)**, and analytical characterization of transmission loss in antenna-embedded walls **(Vähä-Savo et al., 2024)**. Additionally, multi-layer and conformally integrated structurally embedded vascular antenna (SEVA) arrays provide insights into the potential for high-performance, infrastructure-embedded antenna systems **(Bal et al., 2021)**. Empirical formulas for performance prediction of concrete-embedded antennas further support the design and optimization of embedded antenna systems for smart building applications **(Tan et al., 2021)**.

Despite these advances, limited research has addressed direct integration of microstrip antennas into metallic rebar structures, particularly for low-frequency IoT bands. This represents the primary novelty of the current study: combining analytical modeling with fullwave simulations using High Frequency Structure Simulator (HFSS) **(ANSYS Inc, 2023)** to assess return loss, Voltage Standing Wave Ratio (VSWR), gain, and radiation characteristics of microstrip antenna embedded in realistic structural materials. Additionally, leveraging building elements as communication infrastructure can provide secondary benefits, including the use of smart materials and enhanced electromagnetic performance in urban environments.

In summary, this research bridges the gap between microstrip antenna design and practical smart city infrastructure, providing a conceptual framework for scalable, low-visibility, and high-performance IoT communication systems embedded directly within building structures.

2. METHODOLOGY

2.1 Structural and electromagnetic design

The microstrip patch antenna is configured to operate at a center frequency of 700 MHz, targeting the sub-GHz IoT band. The antenna is implemented on an FR4 substrate measuring 170 × 170 mm², with a dielectric constant of 4.4, a thickness of 1.6 mm, and a loss tangent of 0.025. Although FR4 exhibits a relatively high loss tangent, its selection is justified by the fact that the surrounding concrete and steel reinforcement dominate the total electromagnetic losses. Furthermore, FR4 offers significant cost and fabrication advantages over low-loss substrates (e.g., Rogers), making it a pragmatic choice for smart city IoT applications **(Pena et al., 2003) (Sugianto & Hariyadi, 2013)**.

A rectangular ground plane is positioned on the backside of the substrate. The antenna is excited through a 5 mm-wide microstrip line, which provides impedance matching to a 50 Ω feed. The antenna dimensions are calculated using Equations (1) to (4) **(Balanis, 2016) (Surjati, 2010) (Kuravatti, 2018)**. The mathematical formulation utilizes f_c as the design center frequency and c as the speed of light. The dielectric characteristics are expressed through ε_r (material dielectric coefficient) and ε_{eff} (effective dielectric coefficient). The geometric variables Δl and h correspond to the feed line width and substrate height.

The width is determined to optimize radiation efficiency and input impedance:

$$W_p = \frac{c}{2f_c\sqrt{\frac{(\varepsilon_r + 1)}{2}}} \tag{1}$$

Since the electromagnetic fields reside partially in the concrete and partially in the air, the effective dielectric constant must be calculated:

$$\varepsilon_{eff} = \frac{\varepsilon_r + 1}{2} + \frac{\varepsilon_r - 1}{2}\left(\frac{1}{\sqrt{1+12\frac{h}{W}}}\right) \tag{2}$$

The fringing fields at the patch edges cause the antenna to appear electrically longer than its physical length, calculated as:

$$\Delta l = 0.412h\frac{(\varepsilon_{eff}+0.3)\left(\frac{W}{h}+0.264\right)}{(\varepsilon_{eff}-0.258)\left(\frac{W}{h}+0.8\right)} \tag{3}$$

The actual physical length is then derived by adjusting the effective length with the calculated Δl:

$$L_p = \frac{c}{2f_c\sqrt{\varepsilon_{eff}}} - 2\Delta l \quad (4)$$

The finalized design parameters of the suggested microstrip patch antenna are listed in Table 1 and shown in Figure 1.

Table 1. Antenna patch parameters for 700 Mhz center frequency

Parameters	Description	Values (mm)
Lsub	Length of substrate	170
Wsub	Width of substrate	170
Lp	Length of patch	100
Wp	Width of patch	130.4
Lf	Length of feed line	55
Wf	Width of feed line	5
g	Gap of feed line	2
Lg	Length of ground	170
Wg	Width of ground	170

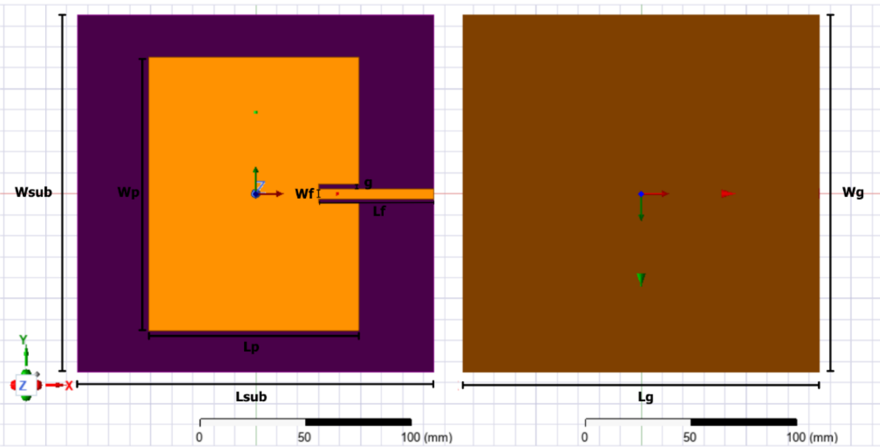

Figure 1. Microstrip antenna design

2.2 Simulation setup

The proposed antenna was designed, simulated, and evaluated using HFSS. This software is selected for its capability to accurately model complex geometries, incorporate material properties, and predict electromagnetic performance under realistic conditions. To improve simulation accuracy, material properties are defined based on construction standards. Adaptive meshing is applied, along with a frequency sweep from 100 MHz to 1400 MHz, to ensure reliable results.

The design process involves integrating a microstrip patch antenna into a concrete column model, where the antenna replaces one stirrup within an arrangement of four reinforcing bars. The surrounding concrete and air domains are assigned appropriate dielectric properties to evaluate their effects on the antenna's resonant frequency, impedance characteristics, and radiation performance. The selection of the relative permittivity (ε_r = 6.5) and loss tangent (tan δ = 0.02) for the concrete is based on an extensive literature review regarding the characteristics of construction materials in the sub-GHz (Low-Band) frequency range **(Zhekov et al., 2020) (Taylor et al., 2022)**. While the ε_r of concrete typically ranges from 4 to 12, a value of 6.5 was chosen as it represents dry concrete with low to moderate moisture content.

This condition is prevalent in established urban structures; thus, ε_r = 6.5 is adopted as the nominal value for realistic steady-state modeling. Furthermore, the loss tangent of 0.02 reflects low dielectric loss, which is heavily influenced by conductivity and moisture. This value falls within a reasonable range for high-quality dry concrete, ensuring that the simulation remains focused on the conductive effects of the steel reinforcement on antenna performance, rather than excessive attenuation from saturated dielectric materials.

The simulation environment features a concrete column enclosed in a radiation air box, where a lumped port serves as the excitation source at the microstrip feed line interface. The antenna is surrounded by an approximately 1 cm vacuum region to minimize immediate interaction with the concrete. This configuration enables accurate evaluation of reflection coefficients and electromagnetic field distributions while considering structural integration. For future experimental validation, the 10 mm air gap can be maintained through a two-step casting process. First, the antenna module is cast in a small mold, where a low-permittivity foam spacer inside a thin-walled plastic box prevents cement paste from filling the gap. After the module has cured, it is placed into the main column mold and cast along with the rest of the concrete. Figure 2 illustrates the simulation model.

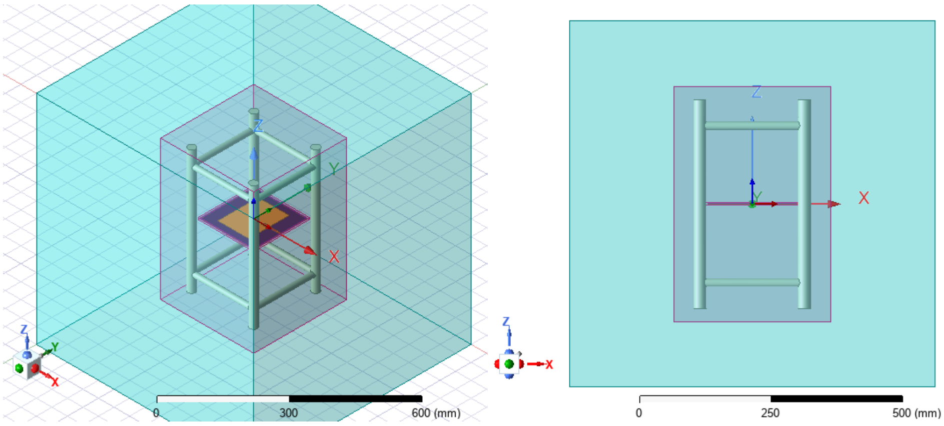

(a) **(b)**

Figure 2. Microstrip-embedded building structure antenna simulation model: (a) Dimetric projection (b) Front view configuration

Table 2. Simulation parameters

Parameters	Values
Target Frequency	700 MHz
Frequency Range	100–1400 MHz
Antenna Type	Microstrip
Antenna Material	Patch: Copper Ground: Copper Substrate: FR4 Epoxy
Air Gap Layer	10 mm
Reinforcing Bar	4 Carbon Steel
Reinforcing Bar Diameter	12 mm
Reinforcing Bar Height	400 mm
Stirrup Diameter	8 mm
Stirrup Height	20 mm
Stirrup Spacing	150 mm
Embedding Medium	Concrete
Boundary Condition	Radiation (Open)
Excitation	Lumped Port 50 Ω

The simulation parameters are summarized in Table 2. These parameters specify the antenna geometry, material composition, boundary conditions, and excitation settings required for accurate modeling within the concrete structure. The chosen configuration is intended to represent realistic construction scenarios and to assess the electromagnetic performance of the embedded antenna under practical conditions.

2.3 Performance metrics

The antenna performance is evaluated based on several key electromagnetic parameters: (1) return loss (S_{11}), to determine resonance frequency and impedance matching characteristics; (2) radiation pattern, to analyze the directional characteristics of the antenna; and (3) gain, to assess power conversion efficiency and its suitability for IoT network.

Table 3. Physical and electromagnetic parameters of materials

Parameters	Patch	Concrete
Relative Permittivity ($\boldsymbol{\varepsilon_r}$)	1	6.5
Relative Permeability ($\boldsymbol{\mu_r}$)	0.99	1.0
Bulk Conductivity (S/m)	5.8×10^7	0.01
Conductivity	Copper	Low Conductivity Cementitious Material
Loss Tangent ($\tan \boldsymbol{\delta}$)	0	0.02
Density (kg/m³)	8933	2400

Metallic and dielectric materials are characterized using physical properties that closely approximate real construction materials, as detailed in Table 3. These parameters serve as a practical basis for future experimental validation and potential implementation in smart city environments. This approach facilitates the evaluation of microstrip-embedded building structure antenna's performance within standard structural geometries and IoT network.

3. RESULTS AND DISCUSSION

This section presents a comprehensive analysis of the microstrip-embedded antenna's performance, correlating theoretical objectives with numerical results obtained via HFSS. The discussion focuses on the electromagnetic interactions between the antenna and its environment, specifically the loading effects of the concrete medium and interference from the steel reinforcement.

3.1 Return loss (S_{11}) and bandwidth

The reflection coefficient (S_{11}) of the microstrip-embedded building structure antenna was simulated to evaluate its impedance matching at the target frequency of 700 MHz. As shown in Figure 3, the antenna exhibits a deep resonance at approximately 700 MHz with a return loss value of -17.15 dB.

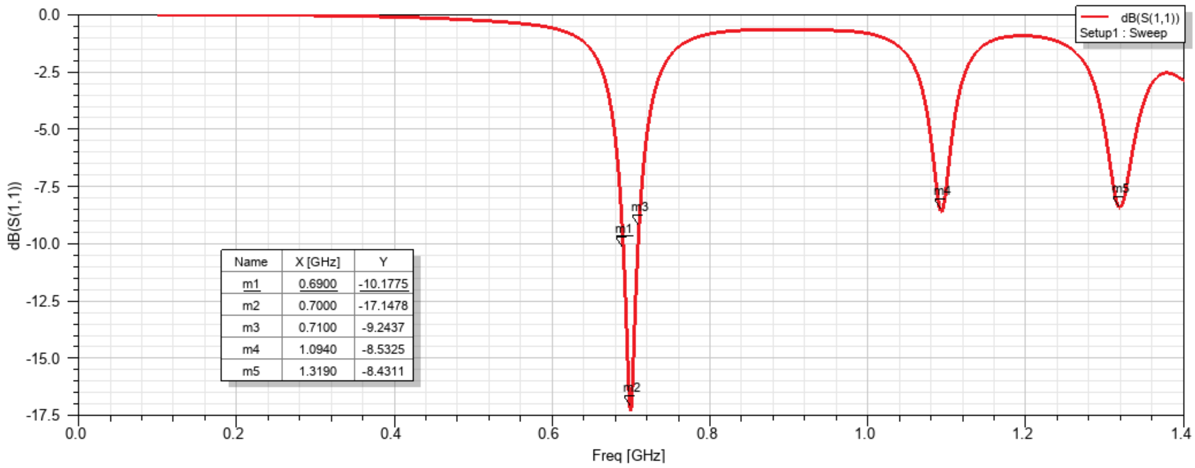

Figure 3. Simulated S_{11} of microstrip-embedded building structure antenna

The reflection coefficient (S_{11}) indicates a robust resonance at the target frequency, with the -10 dB bandwidth observed at 20 MHz, covering the range from 690 MHz to 710 MHz. This slight deviation from the nominal 700 MHz design is attributed to the high permittivity of the surrounding concrete, which increases the effective electrical length of the patch.

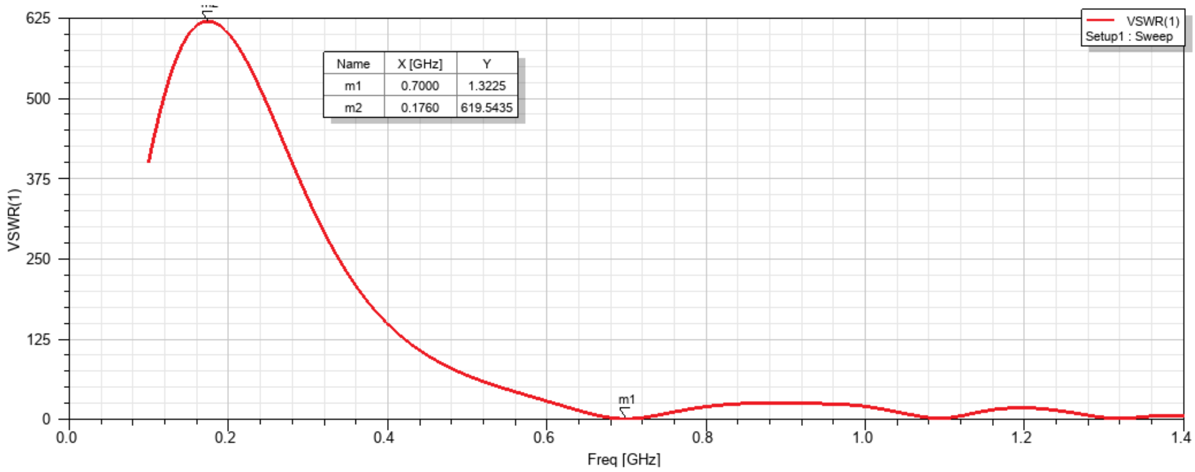

Figure 4. Simulated VSWR of microstrip-embedded building structure antenna

Furthermore, the antenna achieves a Voltage Standing Wave Ratio (VSWR) of 1.32, as shown in Figure 4, demonstrating that the 50 Ω lumped port excitation maintains excellent impedance matching despite the complex electromagnetic environment of the concrete column and carbon steel reinforcements.

3.2 Radiation patterns

The radiation characteristics of the microstrip antenna were analyzed using both 2D polar plots and 3D radiation patterns to evaluate its spatial coverage within the structural medium. The radiation characteristics at 700 MHz, as illustrated in Figure 5, were examined in the E-plane and H-plane, showing that the antenna maintains a predominant broadside radiation characteristic despite being integrated into the concrete.

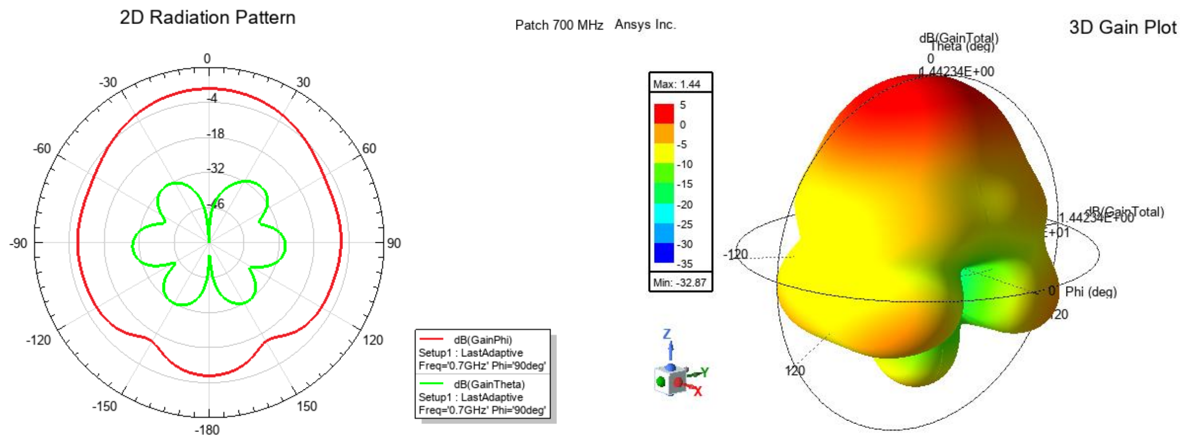

(a) (b)

Figure 5. Radiation Characteristics: (a) 2D Radiation Pattern (b) 3D Gain Plot

The peak radiation intensity is observed at θ = 0° with an achieved front gain of +1.44 dB, confirming that the primary beam remains perpendicular to the microstrip patch surface. Conversely, a significant reduction in gain occurs at the opposite angle, with the back gain decreasing to -6.83 dB at θ = 180°. This indicates that the concrete volume and the internal steel reinforcement act as a physical barrier, effectively suppressing back-radiation and concentrating energy toward the outward-facing hemisphere. While the presence of vertical reinforcing bars and steel stirrups acts as parasitic elements, causing scattering effects and minor nulls in specific angular directions, the antenna maintains a stable main lobe with a Front-to-Back Ratio (FBR) of 8.27 dB. Although the embedded configuration within a dense cementitious environment and carbon steel cage introduces certain distortions compared to a free-space environment, the observed directional coverage and signal penetration confirm the antenna's suitability for urban IoT applications. Building upon these findings, future iterations will prioritize outward-facing alignment through lateral positioning (left/right) to maximize signal penetration, while maintaining the structural integrity of the column by leaving the internal stirrup layout unmodified.

3.3 Antenna gain and efficiency

The simulated maximum realized gain of the microstrip antenna embedded within the concrete column is 1.44 dBi. This gain value is notably lower than that of a standard patch antenna in free space (typically 5-7 dBi), which serves as empirical validation of the significant attenuation caused by the concrete medium and the electromagnetic shadowing effect from the carbon steel reinforcement.

Furthermore, the antenna exhibits a Front-to-Back Ratio (FBR) of 8.27 dB. While the majority of the electromagnetic energy is directed outward, this FBR value suggests the presence of signal scattering and secondary reflections caused by the metallic stirrups and rebar within the column. Despite these losses, the antenna maintains a positive gain over an angular range θ = -22° to +22°. This resulting beamwidth of approximately 44° ensures a stable and reliable communication link for IoT gateways positioned in front of the structural element.

4. CONCLUSION

This research successfully validates a conceptual microstrip antenna embedded within concrete columns for 700 MHz smart city IoT networks via HFSS simulations, confirming that substituting a stirrup's position enables seamless communication integration without compromising resonant characteristics. The antenna exhibits robust performance with a return loss of –17.15 dB, VSWR of 1.32, realized gain of 1.44 dBi, and a broadside radiation pattern, while the 10 mm air gap effectively mitigates electromagnetic interference from the concrete medium. Despite attenuation from reinforcement, the 8.27 dB Front-to-Back Ratio leverages the structure as a natural reflector to enhance outward coverage, offering a space efficient and weather resistant solution for dense urban deployments. The future work is planned to experimentally test physical prototypes to evaluate the impact of concrete moisture fluctuations on real-time frequency stability.

ACKNOWLEDGEMENTS

The authors gratefully acknowledge the availability of Ansys HFSS under an academic research license provided by Department of Electrical Engineering University of Cokroaminoto Makassar, which was instrumental in conducting the electromagnetic simulations presented in this study. This research was funded by the Ministry of Higher Education, Science, and Technology of the Republic of Indonesia, through the Directorate General of Research and Development, under the Basic Research Scheme for the 2025 Fiscal Year, bearing Main Contract No. 130/C3/DT.05.00/PL/2025, dated May 22, 2025.

REFERENCES

Akyıldız, A., & Durmaz, O. (2022). Investigating electromagnetic shielding properties of building materials doped with carbon nanomaterials. *Buildings, 12*(3), 361.

Andalisto, D., Saragih, Y., & Ibrahim, I. (2022). Analisis Kualitatif Teknologi 5G Pengganti 4G di Indonesia. *Jurnal Edukasi Elektro, 6*(1), 01 - 09.

ANSYS Inc. (2023). *HFSS: High frequency structure simulator documentation.* Retrieved from https://www.ansys.com.

Arifin, F. R., Zain, N., & Emakarim, L. R. (2025). Performance Analysis of Building-Embedded Loop Antenna Systems For Smart City Iot Networks. *Jeetech*, *6*(2), 156 - 166.

Bal, A., Baur, J. W., Hartl, D. J., Frank, G. J., Gibson, T., Pan, H., & Huff, G. H. (2021). Multi-Layer and Conformally Integrated Structurally Embedded Vascular Antenna (SEVA) Arrays. *Sensors, 21*(5), 1764.

Balanis, C. A. (2016). *Antenna Theory: Analysis and Design (4th Ed.).* Hoboken, NJ: John Wiley & Sons.

Chen, X., & Zheng, Z. (2023). A Wideband Bow-Tie Slot Antenna Embedded in Dielectric for 5G Communication. *International Conference on Microwave and Millimeter Wave Technology (ICMMT),* (pp. 1 - 3).

Curwen, P., & Whalley, J. (2021). *Understanding 5G Mobile Networks: A Multidisciplinary Primer.* Bingley, UK: Emerald Publishing.

Hussain, R., Alhuwaimel, S. I., Algarni, A. M., Aljaloud, K., & Hussain, N. (2022). A Compact Sub-GHz Wide Tunable Antenna Design for IoT Applications. *Electronics, 11*(7), 1074.

Inclán-Sánchez, L. (2023). Performance Evaluation of A Low-Cost Semitransparent 3D-Printed Mesh Patch Antenna for Urban Communication Applications. *Electronics, 13*(1), 153.

Jusoh, A. Z., Husain, N. F., Abdul Malek, N. F., Mohd Isa, F. N., & Mohamad, S. Y. (2023). Design of Miniaturized Antenna for IoT Applications Using Metamaterial. *IIUM Engineering Journal, 24*(1), 122–137.

Khan, S., Mazhar, T., Shahzad, T., Bibi, A., Ahmad, W., Khan, M. A., Saeed, M. M., & Hamam, H. (2024). Antenna Systems for IoT Applications: A Review. *Discover Sustainability, 5,* 412.

Kumar, N., Kumar, P., & Sharma, M. (2024). Reconfigurable MIMO Antenna for IoT Wireless Applications Controlled by Embedded System. *Journal of Telecommunications and Information Technology, 96*(2), 32–40.

Kuravatti, P. (2018). Comparison of Different Parameters of The Edge Feed and The Inset Feed Patch Antenna. *International Journal of Applied Engineering Research, 13*(13), 11285–11288.

Mehboob, S. A. (2025). Enterprise Architecture Integration for Sustainable Smart Cities: A Comprehensive Framework. *International Journal on Science and Technology (IJSAT), 16*(2), 1–11.

Pavlík, M., Bereš, M., & Beňa, Ľ. (2024). The Influence of Various Commonly Used Building Materials on The Shielding Effectiveness, Reflection and Absorption of The Electromagnetic Wave. *Applied Sciences, 14*(6), 2521.

Pena, D., Feick, R., Hristov, H. D., & Grote, W. (2003). Measurement and Modeling of Propagation Losses in Brick and Concrete Walls for the 900-MHz Band. *IEEE Transactions on Antennas and Propagation, 51*(1), 31–39.

Rita, J., Salvado, J., da Rocha, H., & Espírito-Santo, A. (2025). A Comprehensive Review of IoT Standards: The Role of IEEE 1451 in Smart Cities and Smart Buildings. *Smart Cities, 8*(4), 108.

Sugianto, D., & Hariyadi, T. (2013). Design of Microstrip Antenna for LTE (Long Term Evolution) 700 MHz Applications*. International Conference on Information and Communication Technology (ICoICT),* (pp. 328 - 331).

Surjati, I. (2010). *Antena Mikrostrip: Konsep dan Aplikasi*. Jakarta: Universitas Trisakti.

Tan, J., Shao, Y., Zhang, J., & Zhang, J. (2021). Empirical Formulas for Performance Prediction of Concrete Embedded Antenna. *International Symposium on Antennas and Propagation (ISAP)*, (pp. 201–202).

Taylor, J. M., & Morris, I. M. (2022). Investigating Concrete Properties Using Dielectric Constant from Ground Penetrating Radar Scans. *Infrastructures, 7*(12), 173.

Vähä-Savo, L., Icheln, C., Lü, X., Palermo, A., Marzani, A., & Haneda, K. (2025). Antenna-Embedded Building Elements as Futuristic Cellular Infrastructure: Introduction to A Multiphysics Study. *IEEE Antennas and Propagation Magazine.*

Vähä-Savo, L., Veggi, L., Vitucci, E. M., Icheln, C., Degli-Esposti, V., & Haneda, K. (2024). Analytical Characterization of A Transmission Loss of An Antenna-Embedded Wall. *IEEE Open Journal of Antennas and Propagation, 5*(6), 1765–1772.

Zain, N., Arifin, F. R., & Emakarim, L. R. (2025a). Embedded Metallic Structures As Passive Antennas for Sub-Ghz IoT Communication in Smart City. *International Conference on Research and Innovations in Information and Engineering Technology (RITECH),* (pp. 122–128).

Zain, N., Arifin, F. R., & Emakarim, L. R. (2025b). Transforming Building Infrastructure Into Communication Systems for Smart City: A Conceptual Analysis of Metallic Structures As Antennas. *Journal La Multiapp, 6*(6), 1472–1483.

Zanella, A., Bui, N., Castellani, A., Vangelista, L., & Zorzi, M. (2014). Internet of Things for Smart Cities. *IEEE Internet of Things Journal, 1(*1), 22–32.

Zhekov, S. S., Franek, O., & Pedersen, G. F. (2020). Dielectric Properties of Common Building Materials for Ultrawideband Propagation Studies [Measurements Corner]. *IEEE Antennas and Propagation Magazine, 62*(1), 72–81.